Journal of Applied Fluid Mechanics, Vol. 12, No. 1, pp. 95-102, 2019.
Available online at www.jafmonline.net, ISSN 1735-3572, EISSN 1735-3645.
DOI: 10.29252/jafm.75.253.28840

Numerical Analysis of Homogeneous and Stratified Turbulence under Horizontal Shear via Lagrangian Stochastic Model: Richardson Number Effect

L. Thamri[1,2†], T.Naffouti[1,3,4] and M. Bouzaiane[2,5]

[1] *Université Tunis El-Manar, Faculté des Sciences de Tunis, Département de Physique, Tunisia*

[2] *Laboratoire de Mécanique des Fluides et des Transferts Thermique, Tunisia*

[3] *Laboratoire d'Energétique et des Transferts Thermique et Massique, El Manar 2092, Tunis, Tunisia*

[4] *Institut Préparatoire aux Etudes d'Ingénieurs El-Manar, El-Manar 2092, Tunis, Tunisia*

[5] *Université Tunis Carthage, Faculté des Sciences de Bizerte, Département de Physique, Tunisia*

†*Corresponding Author Email:* thamril@yahoo.fr

(Received January 23, 2018; accepted August 6, 2018)

ABSTRACT

The present investigation is carried out to reveal Richardson number (Ri) effects on an homogeneous and stratified turbulence under horizontal shear. The problem is simulated via Lagrangian Stochastic model (LSM). Hence, the method of Runge Kutta with fourth order is adopted for the numerical integration of three differential systems under non linear initial conditions of Jacobitz (2002) and Jacobitz *et al*. (1998). This study is performed for Ri ranging from 0.2 to 3.0. It has been found that computational results by the adopted model (LSM) gave same findings than that of preceding works. It has been shown a global tendency of different parameters governing the problem to equilibrium asymptotic states for various values of Ri. The comparative study between the computations of the present LSM and direct numerical simulation of Jacobitz demonstrates a good agreement for both methods for the ratios of; potential energy K_θ/E and kinetic energy K/E toward the total energy E and the principal component of anisotropy b_{12} It has been found that Ri is the most important parameter affecting the thermal and dynamic fields of the flow. Hence, increase Ri conduct to increase the uniform stable stratification and decrease for the uniform mean shear S. It can be concluded that Ri is a main non-dimensional parameter which enable us to understand physical phenomenons produced inside stratified shear flows.

Keywords: Richardson number (Ri); Stratified turbulence; Lagrangian Stochastic model; Second orders models; Direct numerical simulation.

NOMENCLATURE

Nomenclature should be in alphabetic order (A – Z) and Greek letters should follow after Latin letters in alphabetic *order (α β ...)*

b	anisotropic tensor of Reynolds
g	constant of gravity
K	turbulent kinetic energy
R_i	Richardson number
S	mean shear
S_ρ	mean scalar gradient
St	non dimensional time ($St = S*t$ (mean shear∗ time))
$\overline{T}_{,i}$	scalar gradient
t	time
u_i	i-th fluctuating velocity component
U_i	i-th mean velocity component
$\overline{U}_{p,q}$	mean speed gradient
$\overline{u_i u_j}$	reynolds stress tensor
$\overline{u_i \theta}$	scalar turbulent flux
x_i	orthonormal Cartesian coordinate system component
ε	terms of dissipation of turbulent kinetic

	energy
θ	fluctuating part of temperature
ρ_0	density of reference
$\overline{\theta^2}$	scalar variance

1. Introduction

Physical phenomenons generated by the development of turbulent flows persist to be an active research area, owing to its importance for fundamental interests, engineering and science applications. The turbulence is encountered in nature and in industry such as atmospheric circulation, turbulent thermal plumes, oceanic and atmospheric mixed layers, geophysical flows, machines and industrial equipments such as pipes, gas turbines, airplanes, etc. Several researchers simulated various complicated problems in order to understand mechanisms governing the turbulence. They prove that is possible to predict characteristics of turbulent flow using theoretical models. The turbulence modeling, as an example Lagrangian Stochastic Model (LSM) enables us to develop better strategies in order to control different problems. Gopalakrishnan *et al*. (1997) applied a Lagrangian particle model to study the dispersion of gas vapour. After that, Changhoon *et al*. (2007) developed a new model of Lagrangian stochastic on the dispersion of dense gas. They investigated the turbulence suppression of stable stratification and obtained results are in good agreement with previous available experimental works. The model adopts a stochastic differential equation for particle movement which based on the global of possible trajectories of fluid particle (Durbin (1980a, 1983)). The diffusion equation for function of probability density of the particle position is explained by the similar process of displacement equation. In this connection, the diffusion equation with LSM is adopted to simulate the particle dispersion of turbulent atmosphere (Durbin *et al*. (1980b), Boughton *et al*. (1987)). Thereafter, LSM based on the Langevin equation is used to analysis the turbulence of atmosphere in particularly trajectories (Wilson *et al*. (1996)). The literature proves that the prediction by diffusion equation is significant than the Langevin equation. For classic numerical approaches and for the Langevin equation integration, Taylor (1921) is the first to apply the Lagrangian description of the transport of homogeneous turbulence. Wilson *et al*. (1981a, 1981b) carried out numerical computations of trajectories of the particle for inhomogeneous turbulence. They compared predicted results with previous experimental study on the problem of atmospheric surface-layer. Also, they focused their investigations on dynamic turbulence. Thomson (1987) and Schiestel *et al*. (1997) initiated enormously necessary criteria for neutral tracer models, resolving many of the difficulties with many models. Consequently and for an atmospheric flow, Lagrangian Stochastic Model can be applied to simulate the problem. Pope (1994) studied the correlation of a second-moment closures and a generalized Langevin approach. In this connection, Langevin approach is necessary an Eulerian stochastic equation that uses a function of probability density closure. It is demonstrated that the importance of the Langevin equation second moment which is a Reynolds stress closure. Therefore, Pope (1994) predicted the correlation between second moment closure model and stochastic model. Durbin *et al*. ((2001), (1994)) are concentrated their attentions on the turbulent flows modelling and second-moment realizability closure.

The aim of this framework is to study the effect of Richardson number (Ri) on homogeneous and stratified turbulence under horizontal shear using the Lagrangian Stochastic Model (LSM). We compare the results of LSM with those of second order models (Thamri *et al*. (2014)) and direct numerical simulation (DNS) of Jacobitz *et al*. ((2002), (1998)).

2. Configuration And Turbulence Modelling

2.1 Physical Problem

In the present study, we analyzed effects of Ri on Lagrangian Stochastic Model (LSM) of homogeneous and stratified turbulence submitted to an horizontal shear (view the bottom fig.1) (Chebbi *et al*. (2012)). Equilibrium states of LSM are investigated in a first step. For a second step, results by LSM are compared with those of second order models and direct numerical simulation (DNS) of Jacobitz (2002).

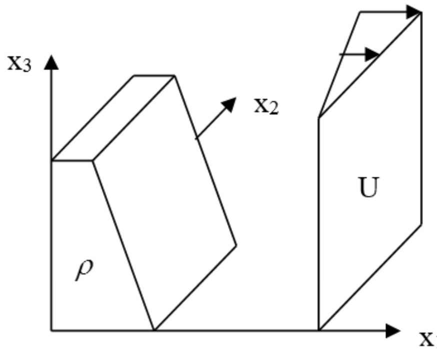

Fig. 1. Schematic of the average density for vertical stratification and the average velocity for horizontal shear at fixed inclination $\theta = \frac{\Pi}{2}$.

2.2 Turbulence Modeling With LSM

Velocity components U_i and the temperature T are defined by the summation of mean and fluctuating values:

$$U_i = \overline{U}_i + u_i$$

$$T = \overline{T} + \theta$$

Lagrangian Stochastic Model (LSM) used in the present investigation is described in details by several researchers (Durbin (1983), Durbin *et al.* (1994), Das *et al.* (2005)). The formulation of LSM is presented by following simple equations:

$$du_i = -\frac{c_1}{2}\frac{\varepsilon}{k}u_i dt + (c_{2\theta}-1)u_k\frac{\partial U_i}{\partial x_k}dt + c_{3\theta}u_k\frac{\partial U_k}{\partial x_i}dt - (1-c_{5\theta})\beta g_i\theta dt + \sqrt{c_0\varepsilon}dW_i \tag{1}$$

$$d\theta = -\left(c_{1\theta} - \frac{c_1}{2}\right)\frac{\varepsilon}{k}\theta dt - (1-c_{4\theta})u_k\frac{\partial T}{\partial x_k}dt + \sqrt{c_\theta}dW_\theta \tag{2}$$

The coefficients c_0 and c_θ are specified as:

$$c_0 = \frac{2}{3}\left[c_1 - 1 + (c_2 + c_3)\frac{P}{\varepsilon} + c_5\frac{G}{\varepsilon}\right] \tag{3}$$

$$c_\theta = -2c_{4\theta}\overline{\theta u_k}\frac{\partial T}{\partial x_k} + \frac{\varepsilon}{k}(2c_{1\theta} - c_1 - R)\overline{\theta^2} \tag{4}$$

Where $c_1 = 1.8, c_2 = 0.6, c_3 = 0.0$ $c_5 = 1/3$, $c_{1\theta} = 2.5, c_{2\theta} = 0.6,$

$c_{3\theta} = 0.0, c_{4\theta} = 0.0,$ $c_{5\theta} = 1/3,$ R=1.5.

For the problem of Warhaft (2000) related to uniform mean scalar gradient, the constant R is about equal to 1.5. In this study, same value of R is adopted.

The present research is simulated for an incompressible fluid by the continuity equation (1), for the density with a transport equation 2 and three dimensional unsteady Navier-Stokes equations with the Boussinesq approximation.

Different equations of transport for: the velocity correlation $\overline{u_i u_j}$, components $\overline{u_i\theta}$ of the scalar turbulent flux, the variance of scalar $\overline{\theta^2}$ and the turbulent kinetic energy K are developed by equation (1) and (2):

$$\frac{d}{dt}\overline{u_i u_j} = -c_1\varepsilon b_{ij} - (c_{2\theta}-1)P_{ij} + \frac{2}{3}(c_2+c_3)P\delta_{ij} - c_{3\theta}D_{ij} + (1-c_{5\theta})G_{ij} + \frac{2}{3}c_5 G\delta_{ij} - \frac{2}{3}\varepsilon\delta_{ij} \tag{5}$$

$$\frac{d}{dt}\overline{u_i\theta} = -c_{1\theta}\frac{\varepsilon}{k}\overline{u_i\theta} + (c_{2\theta}-1)\overline{u_k\theta}\frac{\partial U_i}{\partial x_k} + c_{3\theta}\overline{u_k\theta}\frac{\partial U_k}{\partial x_i} - (1-c_{5\theta})\beta g_i\overline{\theta^2} - (1-c_{4\theta})\overline{u_i u_k}\frac{\partial T}{\partial x_k} \tag{6}$$

$$\frac{d}{dt}\overline{\theta^2} = -2\overline{u_k\theta}\frac{\partial T}{\partial x_k} - R\frac{\varepsilon}{k}\overline{\theta^2} \tag{7}$$

$$\frac{d}{dt}K = \left[\left(c_{2\theta} - 1 - \frac{2}{3}(c_2+c_3)\frac{\partial U_i}{\partial x_k}\right) + c_{3\theta}\frac{\partial U_k}{\partial x_i}\right]b_{ik} - \left[2(1-c_{5\theta}) + \frac{2}{3}c_5\right]F_i - \frac{\varepsilon}{KS} \tag{8}$$

$F_i = \frac{g}{\rho_0}\frac{\overline{u_i\theta}}{KS}$ is the component of the scalar of turbulent flux (Warhaft (2000)). The components b_{ij} is defined by Holt *et al.* (1992) as:

$$b_{ij} = \frac{\overline{u_i u_j}}{2k} - \frac{\delta_{ij}}{3}.$$

2.3 Gradient Richardson Number

In the present paper, we used the method of Runge Kutta with fourth order. This method is adopted for the integration of equations while we use initial condition of the (DNS) of Jacobitz (2002) and Jacobitz *et al.* (1998). Numerical simulations are presented for various gradient Richardson number (Ri) fixed at 0.2, 0.4, 0.6, 1.0 and 3.0 related to weak and strong stratifications. For stratified shear flows, Ri is a significant dimensionless parameter defined by the ratio of the turbulence buoyant by the turbulence shear. It is defined by the following equation:

$$\mathrm{R}i = \frac{N^2}{S^2} = \frac{-g(\partial\rho/\partial x_3)/\rho_0}{S^2}$$

$N^2 = -g(\partial\rho/\partial x_3)/\rho_0$ is the Brunt–Väisäla frequency where x_3 is the vertical coordinate, ρ is the density of fluid, g is the acceleration of gravity, ρ_0 is the reference density.

$S = \frac{\partial U}{\partial x_2}$ is the uniform horizontal mean shear.

3. Results And Discussions

3.1 Richardson Number Effect

Table 1 demonstrate values of asymptotic equilibrium of parameters governing the considered problem for various Ri at fixed initial value of the shear number $(\varepsilon/KS)_0 = 1/2$ reached by LSM.

Fig.2 shows the evolution of the principal component of anisotropy b_{12} as a function of the normalized time St, obtained by (LSM) for different values of the gradient Ri respectively equal to 0.2, 0.4, 0.6, 1.0 and 3.0.

The LSM confirms the presence of states of asymptotic equilibriums for the parameter b_{12}. This model shows that the component $(b_{12})_{\infty}$ decreases with the increasing of Ri ranging from 0.2 to 3.0 corresponding to weak and strong stratifications, respectively. We note also that the influence of Ri

Table 1 Values of asymptotic equilibrium for different parameters at (ε/KS)₀=1/2

Ri	$(b_{12})_\infty$	$(\overline{\theta u_2})_\infty$	$(P/KS)_\infty$	$(\eta)_\infty$	$(K/E)_\infty$	$(K_\theta/E)_\infty$
0.2	-0.123	-0.354	0.246	0.430	0.700	0.300
0.4	-0.125	-0.455	0.250	0.438	0.695	0.305
0.6	-0.126	-0.530	0.252	0.571	0.637	0.363
1.0	-0.127	-0.648	0.254	0.643	0.609	0.391
3.0	-0.130	-1.04	0.260	0.793	0.558	0.442

ranging from 0.2 up to 3.0 for the parameter of anisotropy b_{12} tends towards states of equilibrium states from $St \geq 60$.

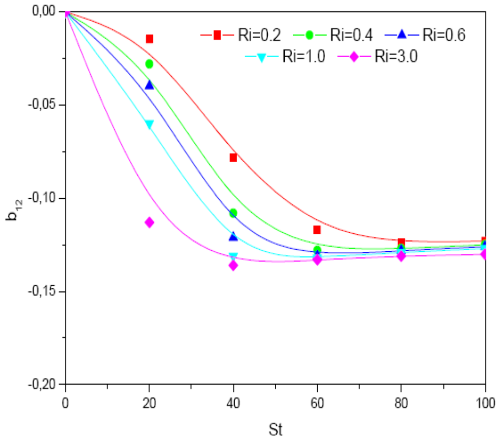

Fig. 2. Temporal evolution of the principal component of anisotropy b12 for different Ri.

For the heat flux $\overline{\theta u_2}$, we note that the results of DNS of Holt *et al.* (1992) showed that for a strong stratification (0.2< Ri <3.0), the heat flux $\overline{\theta u_2}$ changes sign during its evolution. We associated this change a value of Ri name the value of transition. This value is characteristic of the change of state of the turbulence of the state dominated by the shear in a state dominated by gravity.

The temporal evolution of the heat flux $\overline{\theta u_2}$ and $\overline{\theta u_3}$ depicted by LSM for different values of the gradient Ri respectively equal to 0.2, 0.4, 0.6, 1.0 and 3.0 are presented in fig.3 and fig.4, respectively. LSM proves the presence of states of an asymptotic equilibrium for different values of Ri. Furthermore, this model shows that the increase of Ri from 0.2 to 3 decrease the heat flux $\overline{\theta u_2}$ and $\overline{\theta u_3}$.

In fig.5 is shows the time evolution of the non-dimensional ratio η = K_θ/K of potential energy to kinetic energy versus Ri. LSM proves the presence of states of an asymptotic equilibrium for this parameter. For the case of intense stratification related to Ri =1.0 and 3.0, the state of asymptotic equilibrium is obtained more rapidly than that at feeble stratification corresponding to Ri = 0.2, 0.4 and 0.6. In addition, profiles demonstrate that states of asymptotic equilibriums with LSM are slightly dissimilar for strong stratification.

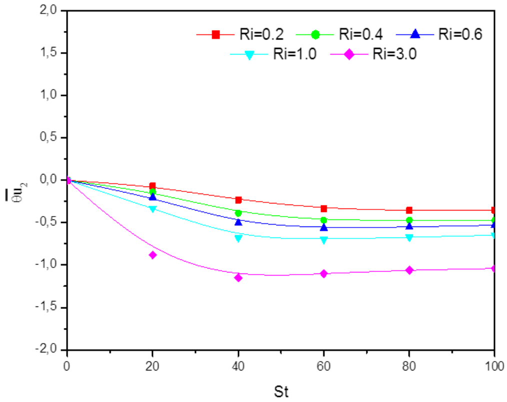

Fig. 3. Temporal evolution of the heat flux $\overline{\theta u_2}$ for different Ri.

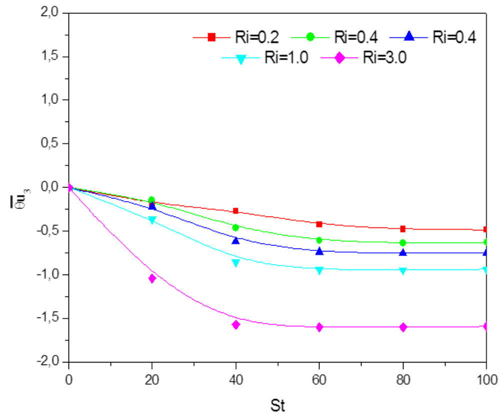

Fig. 4. Temporal evolution of the heat flux $\overline{\theta u_3}$ for different Ri.

For various Ri, the temporal evolution of the component P/KS predicted by the LSM is illustrated in fig.6. Using LSM, it is found that states of the asymptotic equilibrium are obtained for high time and become independent with different Ri. A weak variation is observed for feeble times. Also, LSM shows that the parameter $(P/KS)_{oo}$ increases with as increasing Ri from 0.2 to 3.0. We notice that some is the influence of Ri, the component P/KS tends towards states of equilibrium states from St > 60.

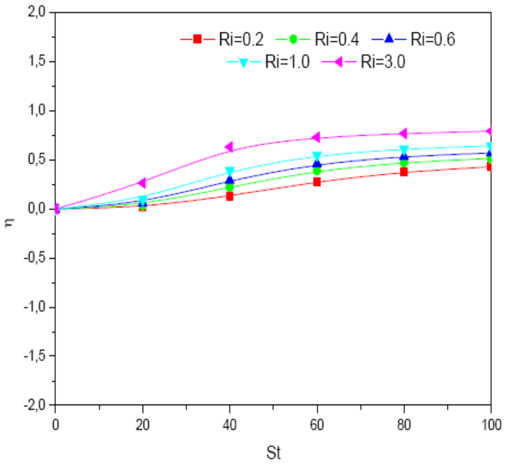

Fig. 5. Temporal evolution of the non-dimensional ratio η versus Ri.

The exchange between the kinetic energy and the potential energy is the essential mechanism controlling the evolution of the vertical heat flux $\overline{\theta u_2}$. It is then interesting to analyse the influence of the Ri on the relationship between two forms of energy. The (DNS) of Holt *et al*. (1992) showed the non-dimensional ratio η = P.E/V.K.E tends towards a constant when St = 100 becomes large for a constant value of Ri. For the heat flux of the gradient type, the vertical kinetic energy is owing to a redistribution of energy through the correlations pressure-deformation. This vertical kinetic energy is converted thereafter into potential energy of which a part is dissipated and η becomes constant.

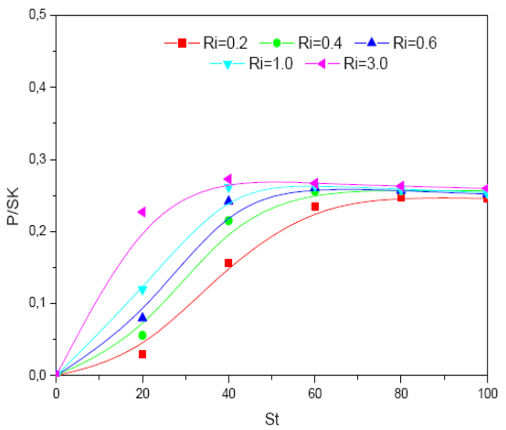

Fig. 6.Temporal evolution of the normalized production P/KS versus Ri.

Temporal variations of ratios kinetic energy to total energy K/E and potential energy to total energy K_θ/E for various Ri are depicted on fig.7 and fig.8, respectively. For high Ri related to strong stratification, it is found that both ratios K/E and K_θ/E are maintained to value 0.5 for higher time St > 40.Hence, states of asymptotic equilibrium of these parameters is detected for intense stratifications. Consequently, the LSM proves an equi-partition of the turbulent kinetic energy and potential energy defined by E=K+K_θ.

In addition, the increase of Ri from 0.2 to 3.0 conducts to decrease the ratio of K/E and to increase the ratio of K_θ/E. It is owing to domination of scalar effect than that the shear effect as increasing Ri from 0.2 to 3.0.

Different ratios are related to the non-dimensional ratio η. They calculated with equations as:

$$\frac{K}{E}=\frac{1}{1+\eta} \text{ and } \frac{K_\theta}{E}=\frac{\eta}{1+\eta}. \tag{9}$$

Different parameters b_{12}, B/ε and ε/KS are calculated by the temporal turbulent kinetic energy K with the equation:

$$\frac{dK}{dSt}=(-2b-F-\frac{\varepsilon}{SK})K \tag{10}$$

For infinite time (St ∞), various parameters are maintained at constant values. For same condition, the equation (10) is defined by a first-order differential equation for constant coefficient as:

$$\frac{dK}{dSt}=\alpha K \tag{11}$$

Where:

$$\alpha_K=2b_{12}-F_3-\frac{\varepsilon}{S.K} \tag{12}$$

For St ∞ , we conclude that

$$K = K(0)\exp(\alpha_K \tau) \tag{13}$$

3.2 Comparison Between Present Work and Direct Numerical Simulation (DNS)

Temporal variations of the component b_{12}, K/E and K_θ/E for three second order models (Thamri *et al*. (2014), SSG-SL (Speziale, Sarkar and Gatski- Shih and Lumley) (Speziale *et al*. (1990), Shih *et al*. (1989), Hechmi *et al*. (2012)), SSG-CL (Speziale, Sarkar and Gatski- Craft and Launder) (Speziale *et al*. (1990), Craft *et al*. (1989)), SSG-LRR (Speziale, Sarkar and Gatski-Launder, Reece and Rodi) (Speziale *et al*. (1990), Launder *et al*. (1975)) and for the LSM, compared with results of Direct Numerical Simulation (DNS) of Jacobitz (2002) are illustrated in figures 9 and 10. It is found that parameters governing the problem b_{12}, ε/KS, K/E and K_θ/E converge to states of asymptotic equilibrium for elevated times. Different results of states of asymptotic equilibrium for various models are illustrated in table 2.

Three second order models (SSG-CL, SSG-SL, SSG-LRR) (Thamri *et al*. (2014)) and LSM consolidate the presence of an asymptotic equilibrium values for parameters governing the problem. In this connection, obtained results show the significant contribution of LSM to predict states of equilibrium in order to characterize the field scalar.

Table 2 Values of asymptotic equilibrium for different parameters at Ri = 0.2

	SSG-CL	SSG-SL	SSG-LRR	LSM (present work)	(DNS) of Jacobitz
$(b_{12})_\infty$	-0.134	-0.078	-0.124	-0.123	-0.130
$(\varepsilon / KS)_\infty$	0.105	0.124	0.093	0.111	0.160
$(K / E)_\infty$	0.907	0.918	0.800	0.700	0.850
$(K_\theta / E)_\infty$	0.092	0.082	0.200	0.300	0.270

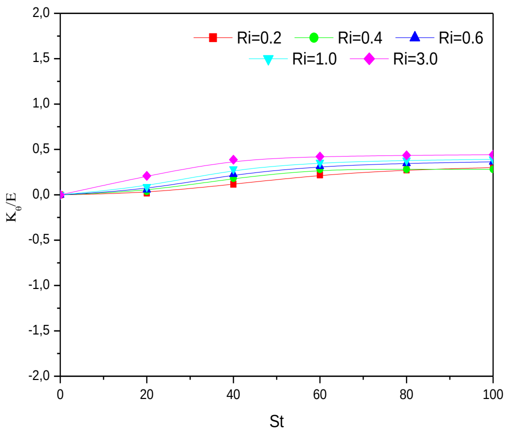

Fig. 7. Temporal evolution of the ratio of kinetic energy to total energy K/E versus Ri.

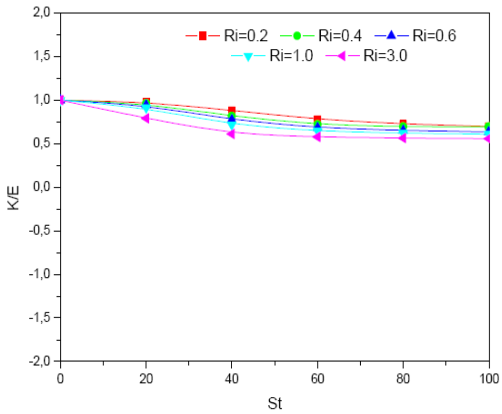

Fig. 8. Temporal evolution of the ratio of potential energy to total energy Kθ/E versus Ri.

Temporal variation of the principal component of anisotropy b_{12} for different models is depicted in Fig.9. It is found that the principal component of anisotropy tends towards states of asymptotic equilibrium for time St beyond 30. In addition, models of LSM, SSG-LRR (Speziale *et al.* (1990), Launder *et al.* (1975)), SSG-CL (Speziale *et al.* (1990), Craft *et al.* (1989)) and DNS of Jacobitz (2002) and Jacobitz *et al.* (1998) show a similar behavior for higher time. A sur-estimation of the values predicted with DNS of Jacobitz is clearly signaled with SSG-SL model (Speziale *et al.* (1990), Shih *et al.* (1989)). For weaker time (St <30), different evolutions are obtained by LSM, second order models (SSG-CL, SSG-SL, SSG-LRR) and DNS of Jacobitz (2002). From figure, it can be concluded a good agreement between results of LSM and DNS of Jacobitz (2002).

Temporal variations of ratios K/E and K_θ/E for various models are illustrated in fig.10. Results corresponding to parameter K/E are similar for SSG-LRR model and DNS of Jacobitz *et al.* (1998) beyond time St $\geq$ 40. Also, predictions by second order models SSG-CL and SSG-SL LSM and DNS of Jacobitz *et al.* (1998) present a same behavior for greater time. For St $\geq$ 40, the LSM shows a sur-estimation of 15% than that DNS of Jacobitz. For the ratio K_θ/E, results related to the LSM and DNS of Jacobitz *et al.* (1998) are in good agreement for time St $\geq$ 35. From this study, it can be concluded that the considerable contribution of the LSM to evaluate states of asymptotic equilibrium for diverse parameters which characterize the problem.

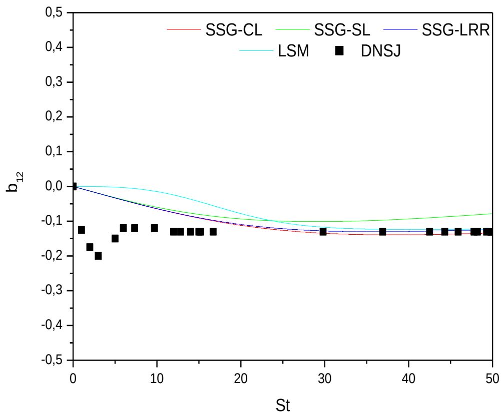

Fig. 9. Temporal evolution of the component b_{12} for various models.

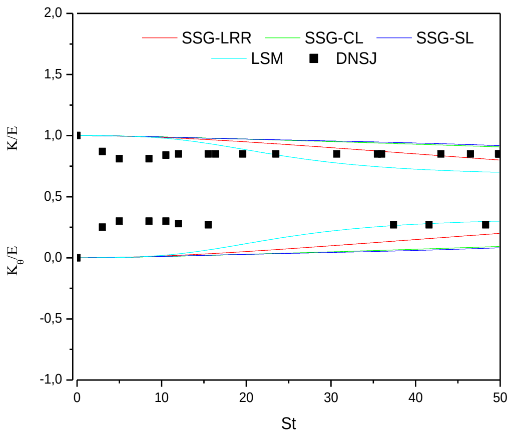

Fig. 10. Temporal evolution of the component K/E and Kθ/E for various models.

4. CONCLUSION

In this investigation, effect of Richardson number (Ri) on homogeneous and stratified turbulence with an horizontal shear using Lagrangian Stochastic Model (LSM) is analyzed. The method of Runge Kutta with fourth order is applied for the numerical integration of three differential systems under initial isotropic state of the DNS of Jacobitz *et al*. (1998) and Jacobitz (2002).

In the first part of this study, it is found that LSM consolidates the presence of states of asymptotic equilibrium for various Ri ranging from 0.2 to 3.0. Consequently, this study proves a significant contribution of LSM in order to determine values of asymptotic equilibrium of different parameter governing the problem such as heat flux ($\overline{\theta u_2}, \overline{\theta u_3}$) turbulent energy (K/E, K_θ/E), principal component of anisotropy (b_{12}), ratio P/KS and η. It is concluded that a correction of various coefficients of LSM by introducing the Ri is considered a significant way to improve the model predictions for diverse parameters. It is considered a border of the Lagrangian modelling adopted in this study.

In the second part of this investigation, results obtained with LSM and DNS of Jacobitz *et al*. (1998) and Jacobitz (2002) demonstrate a good agreement beyond time St > 30.

Finally, the Ri typical of laboratory simulations and DNS of stratified turbulence under an horizontal shear is very important for the developed of the LSM.

We have also shown that the presence of Ri effects in laboratory dispersion or Lagrangian turbulence measurements can cause significant errors (typically of order 25%). This may explain the wide range of values of Ri reported for different turbulent flows.

Stratified turbulence is an active field of research by the raison of various applications in nature and engineering, such as fronts and areas with rough topography, dispersion of pollutants, turbulent phenomenons in atmosphere and aerodynamics domains and oceanic mixing processes.

REFERENCES

Boughton, B. A., J. M. Delaurentis and W. E. Dunn (1987). A stochastic model of particle dispersion in the atmosphere. Boundary-Layer Meteor. 40, 147-163.

Changhoon, L., K. Byung-Gu and K. Suk-Yul (2007). A new Lagrangian stochastic model for the gravity-slumping/spreading motion of a dense gas. *Atmospheric Environment.* 41, 7874–7886.

Chebbi, B. and M. Bouzaiane (2012). On the effects of rotation on the passive scalar and kinematic fields of homogeneous sheared turbulence, *Journal of Applied Fluid Mechanics*. 5(2), 55-65.

Craft, T. J. and B. E. Launder (1989). A model for the pressure scalar gradient correlation and its application to homogeneous and inhomogeneous shear flow.*7th turbulent shear flow, Stanford University press*.12, 1-6.

Das, S. K. and P. A. Durbin (2005). A Lagrangian Stochastic model for dispersion in stratified turbulence. *Phys.Fluid*. 17.

Durbin P. A. (1980a). A random flight model of inhomogeneous turbulent dispersion. *Phys. Fluids*, 23, 2151-2153.

Durbin P. A. and J. C. R. Hunt (1980b). Dispersion from elevated sources in turbulent boundary layers. *J. de M&unique*, 19, 679-695.

Durbin, P. A. (1983). Stochastic differential equations and turbulent dispersion. NASA Reference Publication 19830014275, NASA-RP-1103, E-1425, NAS 1.61:1103. (Available from NTIS as 83N22546).

Durbin, P. A. and B. A. Pettersson-Reif (2001). Statistical Theory and Modeling for Turbulent Flows, Chichester: Wiley. *Journal of Turbulence*. 302, 29-95.

Durbin, P. A. and C. G. Speziale (1994). Realizability of second-moment closure via stochastic analysis. *J. Fluid Mech.* 280, 395-407.

Gopalakrishnan, S.G. and M. Sharan (1997). A Lagrangian particle model for marginally heavy gas dispersion. *Atmospheric Environment*. 31, 3369–3382.

Hechmi, K. and T. Lili. (2012). An Extension of the SSG Model on Compressible Turbulent Flow. *Journal of Applied Fluid Mechanics*. 5, 101-111.

Holt, S. E., J. R. Koseff and J. H. Ferziger (1992). A numerical study of the evolution and structure of homogeneous stably stratified sheared turbulence. *J. Fluid Mech.* 237, 499-539.

Jacobitz, F. and S. Sarkar (1998). The effect of non vertical shear on turbulence in a stably stratified medium. *Phys.Fluid.* 10, 1158-1168.

Jacobitz. F. (2002). A comparaison of the turbulence evolution in a stratified fluid with vertical or horizontal shear. *Journal of Turbulence.* 3, 1-16.

Launder, B. E., G. Reece and W. Rodi (1975). Progress in the developmenty of a Reynolds stress closure. *J. Fluid. Mech.* 68, 537-576.

Pope, S. B. (1994). On the relationship between stochastic Lagrangian models of turbulence and second-moment closures. *Phys. Fluids.* 6, 973.

Schiestel, R. and L. Elena (1997). Modeling of anisotropic turbulence in rapid rotation. *Aerospace Science and Thechnology*. **7**, 441-451.

Shih, T., L. Lumley and J. Chen (1989). Second order modelling of a passive scalar in a turbulent shear flow. *27th Aerospace Sciences Meeting. Center of turbulent Research, Reno, Nevada.*

Speziale, C. G., S. Sarkar and T. B. Gatski (1990). Modeling the pressure strain correlation of turbulence an invariant dynamical systems approach. *NASA Langley research center, Hampton, Virginia*. 2, 3665-5225.

Taylor, G. I. (1921). Diffusion by Continuous Movements, Proceeding of the London Mathematical Society, (2)20, 196-212.

Thamri Naffouti, L., T. lili and M. Bouzaiane (2014). A study of the asymptotic equilibrium behavior in stratified turbulence submitted to an horizontal shear**.** *Journal of Applied Fluid Mechanics (JAFM)*. 7, 401-413.

Thomson, D. J. (1987). Criteria for the Selection of Stochastic Models of Particle Trajectories in Turbulent Flows. *J. Fluid Mech.*. 180, 529-556.

Warhaft, Z. (2000). Passive scalars in turbulent flows. *Annu. Rev. Fluid Mech.* 32, 203-240.

Wilson, J. D. and B. L. Sawford (1996). Review of Lagrangian stochastic models for trajectories in the turbulent atmosphere. Boundary-Layer Meteorol. 78, 191-210.

Wilson, J. D., G. W. Thurtell and G. E. Kidd (1981a). Numerical Simulation of Particle Trajectories in Inhomogeneous Turbulence, III. Comparison of Predictions with Experimental Data for the Atmospheric Surface-Layer, Boundary-Layer Meteorol. 21, 443-463.

Wilson, J. D., G. W. Thurtell and G. E. Kidd (1981b). Numerical Simulation of Particle Trajectories in Inhomogeneous Turbulence. II. Systems with Variable Turbulent Velocity Scale, Boundary-Layer Meteorol. 21, 423-441.